

Influence of the Potassium Chloride Concentration on the Physical Properties of Electrodeposited ZnO Nanowire Arrays

Ramon Tena-Zaera,^{*,†} Jamil Elias,[†] Claude Lévy-Clément,[†] Chegnui Bekeny,[‡] Tobias Voss,[‡] Iván Mora-Seró,[§] and Juan Bisquert[§]

Institut de Chimie et Matériaux de Paris-Est, CNRS, UMR 7182, Bât. F, 2–8 rue Henri Dunant, 94320 Thiais, France, Institute of Solid State Physics, University of Bremen, P.O. Box 330440, 28334 Bremen, Germany, and Departament de Física, Universitat Jaume I, 12071 Castello, Spain

Received: May 23, 2008; Revised Manuscript Received: July 22, 2008

The structural, electrical, and optical properties of zinc oxide nanowire arrays electrodeposited from the reduction of molecular oxygen in aqueous solutions containing zinc chloride and potassium chloride are studied as a function of the potassium chloride concentration. The concentration is varied in a wide range (from 5×10^{-5} to 3.4 M). The evolution of the lattice parameters suggests the formation of zinc interstitials, especially for $[KCl] > 1$ M. The donor density of the as deposited nanowires, which was determined from electrochemical impedance spectroscopy (EIS), varies between 7×10^{18} and $4 \times 10^{20} \text{ cm}^{-3}$. Annealing in air (1 h at 450 °C) decreases the donor density to 10^{17} – 10^{18} cm^{-3} , weakening the dependence on KCl concentration. The line width of the near-band-edge photoluminescence shows a correlation with the donor density. By correlating the variation of the lattice parameters, the donor density and the line width of the photoluminescence, we conclude that intrinsic defects play a dominant role. The incorporation of chlorine impurities appears to be of minor importance, but the concentration of chloride ions in the solution influences the formation of intrinsic defects by modifying the local composition of the electrolyte around the nanowires.

Introduction

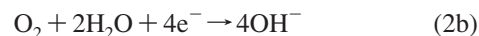
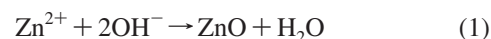
Single-crystal ZnO nanowire arrays have attracted much research interest in the past decade because they not only allow for fundamental studies to improve the understanding of the physical properties of one-dimensional nanostructures but also may be used as building blocks for a new generation of devices in different technological domains such as optoelectronics,^{1,2} solar cells,^{3,4} gas sensing,^{5,6} microfluidics,⁷ field emission,^{8,9} and piezoelectrics.¹⁰

Until now, most of the work has been focused on deposition methods, mainly on those from vapor phase techniques.¹¹ Many pioneering papers on nanostructured devices based on ZnO nanowire arrays can be found in the recent literature.^{1–6,8–10} A precise control of the dimensions and physical properties of the ZnO nanowires is required to increase their performance.

The electrical characterization of nanowire arrays is limited to particular techniques, such as impedance spectroscopy^{12,13} because their morphology complicates the use of more conventional solid-state techniques such as Hall effect measurements. The optical properties of ZnO nanowire arrays have been extensively studied by photoluminescence.^{14–18} Except for some recent works,^{17,19–21} the photoluminescence investigations are mostly focused on nanowire arrays deposited by high-temperature techniques.^{14–16,18}

The potential of ZnO nanowire arrays deposited at low temperatures has been demonstrated in a variety of technological applications.^{2–4,6,7,9} Among the low-temperature deposition techniques, electrodeposition is well-suited to obtain large-scale

ZnO nanowire arrays.²² The controlled ZnO precipitation (eq 1) from the reduction of dissolved molecular oxygen (eq 2a and/or 2b)²³ in zinc chloride solutions²⁴ has been exploited to obtain arrays of ZnO nanowires with tailored dimensions.^{25,26} The concentration of chloride ions (Cl^-) in the electrolyte has been found to be a major parameter to act on the nanowire growth mechanism. This is due to the strong adsorption behavior of Cl^- on ZnO surfaces.²⁷ Since similar approaches have been theoretically studied to attempt the doping in semiconductor crystals,²⁸ the Cl^- concentration is expected to also affect the electrical and optical properties of electrodeposited ZnO nanowire arrays.



Here, we report on a systematic study of the influence of the KCl concentration on the electrical, optical, and structural properties of the electrodeposited ZnO nanowire arrays. By correlating the variation of the lattice parameters, donor density, and PL emission, we conclude that the physical properties of ZnO nanowires are mainly determined by intrinsic defects and that chlorine impurities play a minor role.

Experimental Section

The electrodeposition of ZnO was performed in a three-electrode electrochemical cell with the substrate as the working electrode (cathode), a Pt spiral wire as the counter electrode, and a saturated calomel electrode (SCE) as the reference electrode. The electrolyte was an aqueous solution of ZnCl_2 and KCl, saturated with bubbling oxygen 10 min before and during

* Corresponding author. Fax: +33(0)49781203. E-mail: tena-zaera@icmpe.cnrs.fr.

[†] Institut de Chimie et Matériaux de Paris-Est.

[‡] University of Bremen.

[§] Universitat Jaume I.

the experiment. The ultrapure water (18 M Ω cm) was provided by a Millipore setup. Anhydrous ZnCl₂ salt (Fluka, purity >98.0%) was used as the Zn²⁺ precursor. KCl (Fluka, purity >99.5%) served mainly as a supporting electrolyte.²⁵ The ZnCl₂ concentration was 5×10^{-4} M for all samples and KCl concentration was varied in the range from 5×10^{-2} to 3.4 M. The substrates were commercial conducting (10 Ω /square) glass/SnO₂:F from Solaronix, covered by a thin continuous layer of ZnO deposited by spray pyrolysis at ~ 350 °C.²⁹ The ZnO nanowire arrays were electrodeposited at 80 °C under constant potential (−1 V vs SCE). The charge density was 20 C/cm² for samples deposited using [KCl] \leq 1 M and 5 C/cm² for those obtained with [KCl] > 1 M. On the basis of the results published in ref 25, the charge density was decreased to 5 C/cm² for depositions with [KCl] > 1 M in order to avoid significant differences in the nanowire diameters and in surface-to-volume ratios.

Some samples were annealed in air at 450 °C during 1 h atmospheric pressure using a tubular furnace. The heating ramp was 10 °C/min, and the samples were kept inside the furnace during the cooling.

The morphology and crystalline structure of the ZnO nanowires were analyzed using a Leo 1530 field emission scanning electron microscope (FE-SEM) and a Philips PW1710 powder X-ray diffractometer in Bragg–Brentano configuration. Electrochemical impedance spectroscopy (EIS) measurements were performed in a three-electrode cell using a Pt wire as counter electrode and a standard Ag/AgCl (3 M KCl) as a reference electrode. A carbonate propylene electrolyte (0.1 M LiClO₄) was used to avoid ZnO decomposition. EIS data was obtained using a frequency response analyzer (FRA) equipped PGSTAT-30 from Autolab. Each measurement was done by applying a 20 mV ac sinusoidal signal (frequency ranging between 500 kHz and 5 mHz) superimposed on a constant applied bias. For photoluminescence measurements, a microphotoluminescence setup was used. As excitation source, a frequency-doubled Ti-Sapphire laser with a repetition rate of 82 MHz and a photon energy of 3.542 eV was used for nonresonant excitation. The sample was placed in a cryostat cooled with liquid helium and the temperature was held constant at 7 K. The laser light was focused on the sample through a microscope objective (spot diameter on sample 2 μ m). The photoluminescence from the nanowires was collected via the same objective and spectrally resolved by a spectrometer (resolution of 0.06 nm) equipped with a liquid nitrogen cooled CCD camera.

Results and Discussion

The influence of KCl concentration on the structural, electrical, and optical properties of ZnO nanowires is investigated. The variation of the lattice parameters, donor density, and photoluminescence characteristics of the ZnO nanowire arrays as a function of the potassium chloride concentration in the electrolyte is discussed.

1. Structural Properties. Electrodeposition resulted in highly homogeneous samples, irrespective of the KCl concentration. As an example, Figure 1 shows SEM micrographs of ZnO nanowire arrays deposited using the lowest (Figures 1a,c) and highest (Figures 1b,d) KCl concentrations. The mean values of the nanowire dimensions and the array density were estimated from a statistical evaluation of SEM images²⁷ and are summarized in Table 1. Nanowire diameters in the range between 110 and 150 nm were obtained for all samples. For a constant charge density, an increase of the nanowire length as a function of KCl concentration can be observed. The influence of the

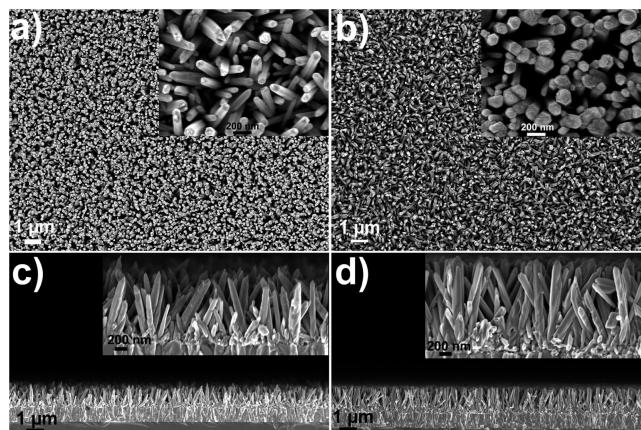


Figure 1. SEM micrographs of ZnO nanowire arrays electrodeposited using [KCl] = 5×10^{-2} M (a, plane view; c, cross section) and [KCl] = 3.4 M (b, plane view; d, cross section). The insets show high-magnification SEM micrographs.

TABLE 1: Mean Values of the Nanowire Dimensions and Array Density for Different KCl Concentrations

[KCl] (M)	diameter (nm)	length (μ m)	density (nanowires cm ⁻²)
0.05	115	0.8	2.3×10^9
0.1	110	1.3	1.8×10^9
0.5	130	2.3	2.0×10^9
1	140	3.2	1.6×10^9
2	110	1.4	2.4×10^9
3.4	140	1.5	2.1×10^9

chloride concentration on the dimensions of the ZnO nanowires have been discussed previously.²⁵

X-ray diffraction (XRD) patterns of ZnO nanowire arrays showed well-defined peaks belonging to ZnO wurtzite phase³⁰ for all analyzed KCl concentration, without spurious phases observed. The XRD patterns were evaluated using the Fullprof software in profile matching mode.³¹ Rietveld refinement was not performed, because the main goal was to obtain precise values of lattice parameters without paying special attention to structure factors and preferential orientation degree. Experimental XRD patterns were fitted and a good agreement was obtained (Figure 1 of Supporting Information). Figure 2 summarizes the evolution of lattice parameters as a function of KCl concentration for as-deposited and annealed ZnO nanowires. Both lattice parameters (*a* and *c*) increase with KCl concentration for the as-deposited samples, the *a* parameter increasing quite gradually. For the *c* parameter, an abrupt increase is observed for [KCl] > 1 M. No significant variations of the *a* parameter were observed after the annealing process. However, annealing resulted in substantial variations of the *c* parameter in nanowires deposited using [KCl] > 1 M. As a result, *c* is approximately constant for all annealed samples, irrespective of the KCl concentration, showing a good agreement with the value reported for standard ZnO (*c*₀ = 5.2066 Å³⁰).

Previous studies have shown that the deposition efficiency, defined as the ratio between the OH[−] ions that reacted with Zn²⁺ (yielding ZnO, eq 1) and the total amount of OH[−] produced from O₂ electroreduction (eq 2a), increases from 3 to 40% by varying KCl concentration between 5×10^{-2} and 3.4 M.²⁵ This suggests that the increase of KCl concentration results in an increase of the [Zn²⁺]/[OH[−]] ratio around the nanowires.²² Since the formation energies of intrinsic defects in ZnO (such as oxygen vacancies (V_O) or zinc interstitials (Zn_i)) decrease under zinc rich conditions,^{32,33} a higher [Zn²⁺]/[OH[−]] ratio may

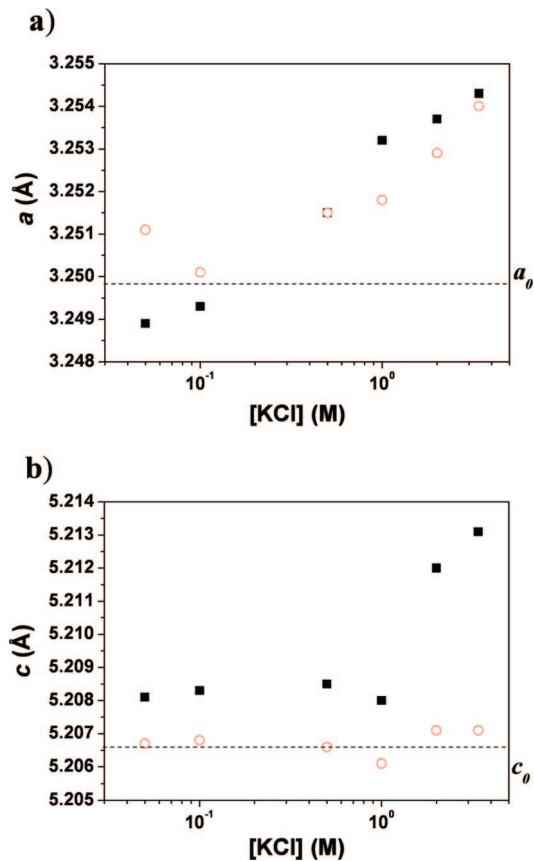


Figure 2. Lattice parameters, determined from X-ray diffraction patterns, of the as-deposited (filled squares) and annealed (open circles) ZnO nanowires as a function of KCl concentration. a_0 and c_0 are the values of the lattice parameters for standard ZnO.³⁰

result in a larger amount of V_O and Zn_i in ZnO nanowires. Theoretical calculations predict the incorporation of Zn_i along the c -axis, inducing a large variation of the c parameter.³⁴ A correlation between the c parameter and Zn_i can be also inferred from recent experimental work in ZnO and $Zn_{1-x}Co_xO$ thin films.³⁵ Accordingly, Zn_i could be the main origin of the increased c parameter, especially for nanowires obtained using $[KCl] > 1$ M. Because the migration of Zn_i should be fast at the annealing temperature (450 °C),^{34,36,37} the decrease of the c parameter after annealing supports this interpretation. The expansion of the a parameter with KCl concentration and its stability under the annealing conditions could be related to the incorporation of chlorine impurities into the ZnO lattice, which should be less sensitive to the annealing treatment.

2. Electrical Properties. Electrochemical impedance spectroscopy (EIS) was used to investigate the donor density of the ZnO nanowire arrays. A Mott–Schottky (MS) model was developed to determine the carrier density in the ZnO samples.¹² This method is an extension of the MS analysis commonly used to determine both dopant density and flatband potential of semiconductor layers and planar semiconductor/liquid junctions, which now takes into account the special geometry of the ZnO nanowires. Solving the Poisson equation, the potential difference across the semiconductor space–charge region, V_{sc} , can be calculated (see Figure 3a):

$$V_{sc} = \frac{qN_D}{2\epsilon} \left[\frac{1}{2}(x^2 - R^2) + x^2 \ln\left(\frac{R}{x}\right) \right] \quad (3)$$

The positive charge in a cylinder of length L is $Q = qN_D\pi(R^2 - x^2)L$ and in the whole array $Q_{tot} = qN_D\pi(R^2 - x^2)LD_{nw}S$,

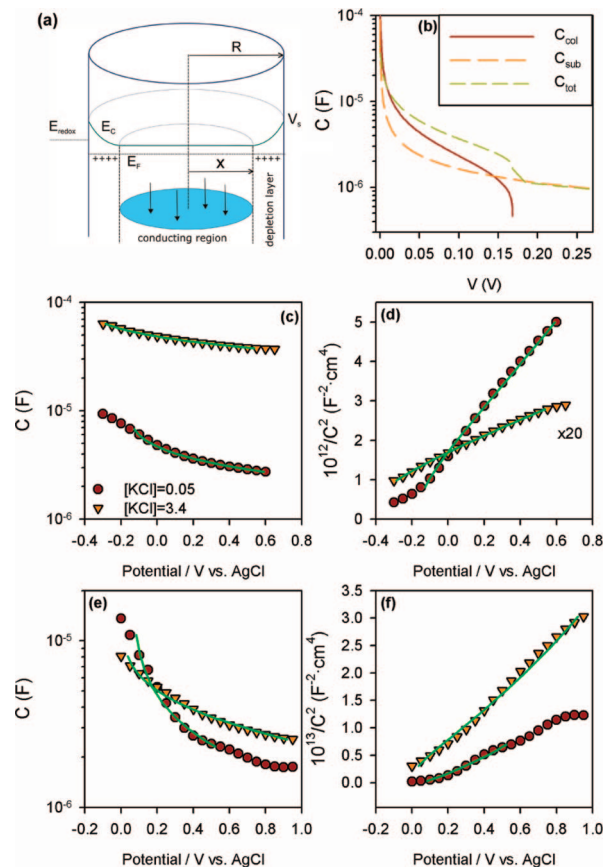


Figure 3. (a) Schematic energy diagram in the radial direction of a nanowire indicating the depletion layer at the surface and the quasineutral region of radius x in the center. V is the potential, V_{sc} is the potential drop across the depletion layer, E_c is the lower edge of the conduction band, and E_F is the Fermi level. (b) Simulation of nanowire array capacitance C_{nw} ($L = 2 \mu\text{m}$, $R = 50 \text{ nm}$, $D_{nw} = 2 \times 10^9 \text{ cm}^{-2}$, $S = 1 \text{ cm}^2$) considering $V = 0 \text{ V}$ as the flat band potential. Complete depletion of nanowires can be observed around 0.17 V vs Ag/AgCl, substrate capacitance $C_{sub} = 5 \times 10^{-7} \text{ V}^{-0.5}$ and total capacitance $C_{tot} = C_{nw} + C_{sub}$. (c and e) Capacitance plots for as deposited and annealed samples, respectively. (d and f) Mott–Schottky plots for as deposited and annealed ZnO nanowire arrays respectively obtained using the lowest ($5 \times 10^{-2} \text{ M}$) and the highest (3.4 M) KCl concentrations. The solid lines represent the fits.

where D_{nw} is the nanowire density per flat surface unit and S is the total flat surface. Computing dV_{sc}/dx and dQ_{tot}/dx , we obtain the capacitance of the nanowire array, dQ_{tot}/dV_{sc} , as a function of the radius of the neutral region x :

$$C_{tot} = \frac{2\pi\epsilon LD_{nw}S}{\ln\left(\frac{R}{x}\right)} \quad (4)$$

The nanowire capacitance was obtained from the impedance spectra. The donor density was determined by fitting the capacitance in that range of voltages where it is governed by the size of the depletion region employing eqs 3 and 4 and taking into account the geometrical characteristics of the sample analyzed.

Parts c and d of Figure 3 show the measured capacitance and MS plots, respectively, for as-deposited samples using the lowest (0.05 M) and the highest (3.4 M) KCl concentration. The solid lines represent the results of the fits. For as-deposited samples (high donor densities), the MS plot shows a linear behavior similar to that typically observed in flat samples.³⁸ The annealed samples (Figure 3e,f) exhibit lower capacitances as a

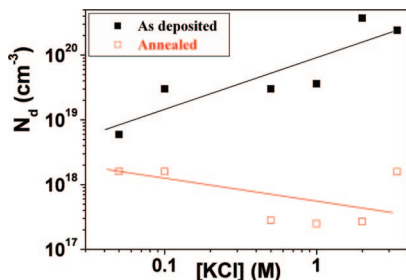


Figure 4. Donor density, determined from electrochemical impedance spectroscopy, of as-deposited (filled squares) and annealed (open squares) ZnO nanowires as a function of KCl concentration. Solid lines are drawn to guide the eye.

consequence of the reduced donor densities. A curved MS plot is obtained, and the effect of the special nanowire morphology is clearly manifested.¹² The annealed sample prepared using [KCl] = 3.4 M shows a step in the capacitance at 0.5–0.6 V vs Ag/AgCl (Figure 3e). This can be better seen in the MS representation (Figure 3f). It is worth noting that a complete depletion of the nanowires was observed for all annealed samples (when N_D is relatively low it is possible to completely deplete the nanowire). Its capacitance becomes rather low in this case, because the variation of the charge with the potential is very small. The effect of nanowire depletion producing a step on the capacitance pattern is shown in Figure 3b, where the substrate capacitance has been also taken into account. Unfortunately, a fit that considers that the capacitances of the nanowires (eqs 3 and 4) and the substrate ($C_{\text{sub}}^{-2} \propto V$) are in parallel cannot be obtained by the conventional ways. As a consequence, we only fitted the experimental points for which the capacitance is mainly governed by the capacitance of the nanowire array (Figure 3e,f). In this case, the model slightly overestimates the N_D value when N_D is low enough. In the most general case, other effects as trap levels could also influence the capacitance pattern.

Figure 4 summarizes the evolution of the donor density as a function of the KCl concentration for the as-deposited and annealed samples. For the as-deposited nanowires, the donor density increases from values slightly lower than 10^{19} cm^{-3} to those higher than 10^{20} cm^{-3} as a function of KCl concentration. A slight decrease of the donor density as a function of KCl concentration is observed for annealed samples.

Because Zn_i act as donors,^{39,40} they could be the main origin of the increased donor densities especially for [KCl] > 1 M. This is in good agreement with the variation of the c parameter as a function of KCl concentration in the as-deposited samples (Figure 2b). Because of their higher mobility, the annealing should affect Zn_i -related defects more strongly than chlorine-related ones. Therefore, we expect chlorine-related impurities to be the dominant remaining donor species in the annealed samples. However, as the donor density of the annealed nanowires measured with EIS shows only a weak dependence on KCl concentration, chlorine-related impurities do not seem to significantly contribute to the electrically active shallow donors in the electrodeposited ZnO nanowires.

3. Photoluminescence. The photoluminescence (PL) spectra measured at 7 K were dominated by the near-band-edge (NBE) emission, while the broad deep level emission (DLE) centered at $\sim 2.1 \text{ eV}$ was distinctly weaker with an intensity ratio $I_{\text{NBE}}/I_{\text{DLE}}$ of about 10 (Figure 2 of Supporting Information). We focus the analysis on the NBE emission to get information about the shallow donors influencing the optical spectra. Figure 5 shows the high resolution PL spectra, recorded in the spectral range

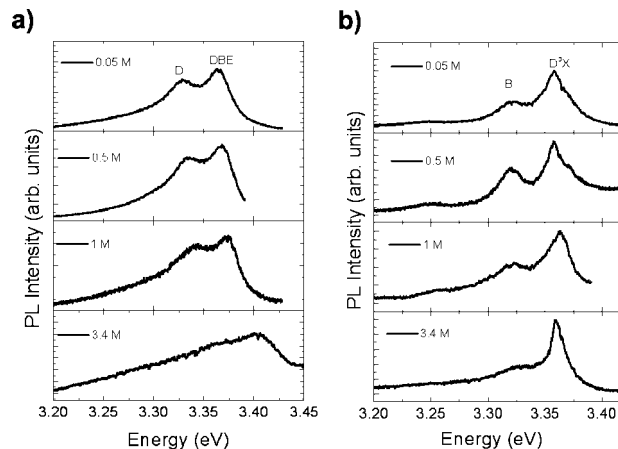


Figure 5. High-resolution photoluminescence spectra, measured at 7 K, of the as-deposited (a) and annealed (b) ZnO nanowire arrays as a function of KCl concentration.

between 3.15 and 3.40 eV, for arrays deposited using different KCl concentration. For the as deposited samples (Figure 5a), two peaks in NBE emission can be clearly observed for [KCl] $\leq 1 \text{ M}$: the DBE (donor band emission) and the D band. Both bands merge for [KCl] > 1 M and only a broad, asymmetric, and structureless spectrum is observed for nanowires deposited using [KCl] > 1 M. For the nanowires deposited at the lowest KCl concentration, the DBE has a line width of 18 meV. Due to the relatively broad line width and the absence of distinguished and relatively sharp emission bands together with the high donor density measured for this sample, the observed emission is attributed to emission from a band of donor states.^{17,41} Detailed and systematic PL investigations of electrodeposited ZnO nanowires revealed that the intensity of the D band scales with the diameter of the nanowires. Therefore, Voss et al.⁴¹ assigned the D band to recombination processes involving surface states. Because the intensity ratio $I_{\text{DBE}}/I_{\text{D}}$ seems to decrease with KCl concentration, a contribution from chloride adsorbates onto the surface of ZnO nanowires is suggested. Nevertheless, the contribution from other adsorbed species cannot be rule out.

As the KCl concentration increases, the line width of the DBE also increases accompanied by a shift of the DBE peak to higher energies (see Table 2). It is important to note that the blue shift goes along with an increase in the donor density determined for the as-deposited nanowires. The discussions about the electrical properties (section 2) led to the conclusion that for higher KCl concentration more Zn_i are incorporated and act as donors in the nanowires. Therefore, the blue shift of the DBE peak with an increase in donor density is due to the filling of lower states in the conduction band (the Burstein-Moss effect).⁴¹

The near-band-edge PL spectra of the annealed samples exhibit two distinguished bands, labeled as B and the D^0X , irrespective of the KCl concentration. The B band is observed at $\sim 3.318 \text{ eV}$ for all annealed samples, while the position of the D^0X emission varies (see Table 2). It must be mentioned that other features can be inferred from these spectra, especially at ~ 3.25 and $\sim 3.375 \text{ eV}$. Small contributions of the peak at 3.375 eV to the main D^0X emission complicate the determination of the line width of the D^0X emission. A clear shift of the main near-band-edge emission and an appreciable reduction of the line width are observed after the annealing process. These results coincide with a reduction of the donor density of the annealed samples. Therefore, we attribute the near-band-edge recombination processes in the annealed samples to result from

TABLE 2: Energy Position and Line Width of the DBE Photoluminescence Emission for the As-Deposited and Annealed ZnO Nanowire Arrays^a

[KCl] (M)	PL				
	as deposited		annealed	N _D (cm ⁻³)	
	E _{DBE} (eV)	FWHM _{DBE}	E _D ⁰ X (eV)	as deposited	annealed
0.05	3.363	18	3.359	5.9 × 10 ¹⁸	1.6 × 10 ¹⁸
0.5	3.366	19	3.358	3.0 × 10 ¹⁹	2.8 × 10 ¹⁷
1	3.372	26	3.362	3.6 × 10 ¹⁹	2.5 × 10 ¹⁷
2	3.378	30	3.357	3.7 × 10 ²⁰	2.7 × 10 ¹⁷
3.4	3.400		3.360	2.4 × 10 ²⁰	1.4 × 10 ¹⁸

^a The values of the donor density, determined from electrochemical impedance spectroscopy, are also shown.

localized excitonic transitions (donor-bound excitons). A detailed discussion concerning this phenomenon and a correlation of the electrical and optical properties of the ECD nanowires can be found elsewhere.⁴¹ The reduction in donor density is most probably due to the out-diffusion of the Zn_i during the annealing process, as discussed in section 2.

By analyzing the variation of the lattice parameters, the donor density, and the near-band-edge PL emission as a function of KCl concentration, we can conclude that [KCl] ≥ 1 M induces the formation of more intrinsic defects (most probably Zn_i) that act as electrical donors. The nature of the main PL peak (DBE) is clearly affected by the concentration of these defects. Annealing at 450 °C in air (1 h) is an effective way to decrease the carrier density to ~5 × 10¹⁷ cm⁻³, resulting in a reduction of the DBE line width. The evolution of the D peak as a function of KCl concentration seems to indicate its relation with chloride adsorbates on the ZnO nanowire surfaces. As suggested by the expansion of the *a* parameter, some chlorine atoms might be incorporated into the ZnO lattice. Nevertheless, their amount should be low compared to the chloride concentration in the deposition solution. This suggests the presence of a “self-purification” process of ZnO nanowires during the electrodeposition because chloride adsorption affects their growth,^{22,25,27} but chlorine impurities do not remain in the ZnO lattice. A potential mechanism for the “self-purification” process could be the formation of zinc–chloride complexes that are generally highly water-soluble. Their dissolution would decrease the chlorine content in ZnO nanowires. Chlorine impurities (adsorbed onto ZnO surfaces and/or placed into ZnO lattice) seem to play a minor electrical role that is not yet fully understood. Because an increase of the [Zn²⁺]/[OH⁻] ratio can be induced by increasing KCl concentration,²² an increase of the Zn_i amount is expected for the highest KCl concentration. The contribution of Zn_i to the high donor density in as-deposited ZnO nanowire arrays is supported by the thermal annealing effects.

Conclusions

A systematic study of the variation of the structural, electrical, and optical properties of the electrodeposited ZnO nanowire arrays as a function of the potassium chloride concentration in the range from 5 × 10⁻⁵ to 3.4 M in the growth solution has been performed. The variation of the lattice parameters before and after annealing has suggested the presence of zinc interstitials, especially for [KCl] > 1. The donor density at room temperature has been determined from electrochemical impedance spectroscopy measurements. The near-band-edge photoluminescence emission has been investigated, yielding a clear correlation between the variation of the donor density and the line width of main PL emission. The electrical and optical properties seem to be mainly determined by intrinsic defects, leaving a minor contribution of chlorine impurities. However,

the chloride concentration is a major parameter that affects the local concentration around the nanowires during the electrodeposition and therefore the formation of intrinsic defects. As a result, the donor density of electrodeposited ZnO nanowires can be modified in a wide range (from 3 × 10¹⁷ to 4 × 10²⁰ cm⁻³) by changing the KCl concentration and postdeposition thermal annealing treatments.

Acknowledgment. The work was partially supported by Ministerio de Educación y Ciencia of Spain under projects HOPE CSD2007-00007 (Consolider-Ingenio 2010) and Generalitat Valenciana under the project GV061347.

Supporting Information Available: Some PL spectra and XRD data. This material is available free of charge via the Internet at <http://pubs.acs.org>

References and Notes

- Park, W. I.; Yi, G. C. *Adv. Mater.* **2004**, *16*, 87.
- Könenkamp, R.; Word, R. C.; Godinez, M. *Nano Lett.* **2005**, *5*, 2005.
- Lévy-Clément, C.; Tena-Zaera, R.; Ryan, M. A.; Katty, A.; Hodes, G. G. *Adv. Mater.* **2005**, *17*, 1512.
- Law, M.; Greene, L. E.; Johnson, J. C.; Saykally, R.; Yang, P. *Nat. Mater.* **2005**, *4*, 455.
- Tien, L. C.; Sadik, P. W.; Norton, D. P.; Voss, L. F.; Pearton, S. J.; Wang, H. T.; Kang, B. S.; Ren, F.; Jun, J.; Lin, J. *J. Appl. Phys. Lett.* **2005**, *87*, 222106.
- Liao, L.; Lu, H. B.; Li, J. C.; He, H.; Wang, D. F.; Fu, D. J.; Liu, C.; Zhang, W. F. *J. Phys. Chem. C* **2007**, *111*, 1900.
- Badre, C.; Pauporté, T.; Turmine, M.; Lincot, D. *Nanotechnology* **2007**, *18*, 365705.
- Wang, X.; Zhou, J.; Lao, C.; Song, J.; Xu, N.; Wang, Z. L. *Adv. Mater.* **2007**, *19*, 1627.
- Ye, C.; Bando, Y.; Fang, X.; Shen, G.; Golberg, D. *J. Phys. Chem. C* **2007**, *111*, 12673.
- Wang, X.; Song, J.; Liu, J. Z.; Wang, L. *Science* **2007**, *316*, 102.
- Yi, C. C.; Wang, C.; Park, W. I. *Semic. Sci. Technol* **2005**, *20*, S22–S34, and references therein.
- Mora-Sero, I.; Fabregat-Santiago, F.; Denier, B.; Bisquert, J.; Tena-Zaera, R.; Elias, J.; Lévy-Clément, C. *Appl. Phys. Lett.* **2006**, *89*, 203117.
- Wu, J. J.; K-P, D. *Adv. Mater.* **2007**, *19*, 2015.
- Park, W. I.; Kim, D. H.; Jung, S. W.; C, G. Y. *Appl. Phys. Lett.* **2002**, *80*, 4232.
- Wischnmeier, L.; Voss, T.; Rückmann, I.; Gutowski, J.; Mofor, A. C.; Bakin, A.; Waag, A. *Phys. Rev. B* **2006**, *74*, 19.
- Xiang, B.; Wang, P.; Zhana, X.; Dayeh, S. A.; Aplin, D. P. R.; Soci, C.; Yu, D.; Wang, D. *Nano Lett.* **2007**, *7*, 323.
- Bekeny, C.; Voss, T.; Gafsi, H.; Gutowski, J.; Postels, B.; Kreye, M.; Waag, A. *J. Appl. Phys.* **2006**, *100*, 103417.
- Zhou, H.; Wissinger, M.; Fallert, J.; Hauschild, R.; Stelzl, F.; Klingshirn, C.; Kaltz, H. *Appl. Phys. Lett.* **2007**, *91*, 181112.
- Bekeny, C.; Voss, T.; Hilker, B.; Gutowski, J.; Hauschild, R.; Kalt, H. B.; Postels, A.; Bakin, A.; Waag, A. *J. Appl. Phys.* **2007**, *102*, 049908.
- Cao, B.; Li, Y.; Duan, G.; Cai, W. *Cryst. Growth Design* **2006**, *6*, 1091.
- Pauporté, T.; Lincot, D.; Viana, B.; Pellé, F. *Appl. Phys. Lett.* **2006**, *89*, 233112.

- (22) Tena-Zaera, R.; Elias, J.; Lévy-Clément, C.; Mora-Sero, I.; Luo, Y.; Bisquert, J., *Phys. Status Solidi A* **2008**, in press (doi: 10.1002/pssa.200779426).
- (23) Strbac, S.; Adzic, R. R. *Electrochim. Acta* **1996**, *41*, 2903.
- (24) Peulon, S.; Lincot, D. *J. Electrochem. Soc.* **1998**, *145*, 864.
- (25) Tena-Zaera, R.; Elias, J.; Wang, G.; Lévy-Clément, C. *J. Phys. Chem. C* **2007**, *111*, 16706.
- (26) Elias, J.; Tena-Zaera, R.; Lévy-Clément, C. *J. Electroanal. Chem.* **2008**, *621*, 171.
- (27) Elias, J.; Tena-Zaera, R.; Lévy-Clément, C. *J. Phys. Chem. C* **2008**, *112*, 5736.
- (28) Erwin, S. C.; Zu, L.; Haftel, M. I.; Efros, A. L.; Kennedy, T. A.; Norris, D. J. *Nature* **2005**, *436*, 91.
- (29) Elias, J.; Tena-Zaera, R.; Lévy-Clément, C. *Thin Solid Films* **2007**, *515*, 8553.
- (30) Powder Diffraction File 00-036-1451, PDF-2 Database Sets, International Center for Diffraction Data Newton Square, PA, 1993.
- (31) Rodriguez-Carvajal, J. *Abstracts of the Satellite Meeting on Powder Diffraction of the XV Congress of the IUCr*, Toulouse, 1990; p 127.
- (32) Zhang, S. B.; Wei, S. H.; Zunger, A. *Phys. Rev. B* **2003**, *63*, 75205.
- (33) Kohan, A. F.; Ceder, G.; Morgan, D.; Van de Walle, C. G. *Phys. Rev. B* **2000**, *61*, 15019.
- (34) Janotti, A.; Van der Walle, C. *Phys. Rev. B* **2007**, *76*, 165202.
- (35) MacManus-Discroll, J. L.; Khare, N.; Liu, Y.; Vicker, M. E. *Adv. Mater.* **2007**, *19*, 2925.
- (36) Vlasenko, L. S.; Watkins, G. D. *Phys. Rev. B* **2005**, *69*, 115212.
- (37) Look, D. C.; Farlow, G. C.; Reunchan, P.; Limpumngong, S.; Zhang, S. B.; Nordlund, K. *Phys. Rev. Lett.* **2005**, *95*, 225502.
- (38) Sze, S. M. *Physics of Semiconductor Devices*, 2nd ed; John Wiley and Sons: New York, 1981; p 79.
- (39) Look, D. C.; Hemsley, J. W.; Szelove, J. R. *Phys. Rev. Lett.* **1999**, *82*, 2252.
- (40) Ozgur, U.; Alivov, Y.; Liu, C.; Teke, A.; Reshchikov, M.; Dogan, S.; Avrutin, V.; Cho, S. J.; Morko, H. *J. Appl. Phys.* **2005**, *98*, 041301.
- (41) Voss, T.; Bekeny, C.; Gutowski, J.; Tena-Zaera, R.; Elias, J.; Lévy-Clément, C.; Mora-Sero, I.; Bisquert, J. *Nanotechnology*. Submitted.

JP804563A